Exhibit 2

Correlative polarizing light and scanning electron microscopy for the assessment of talc in pelvic region lymph nodes

Sandra A. McDonald, Yuwei Fan, William R. Welch, Daniel W. Cramer, Rebecca C. Stearns, Liam Sheedy, Marshall Katler & John J. Godleski

View supplementary material 🗗

Published online: 21 Mar 2019.

Submit your article to this journal 🗗

View Crossmark data 🗗

Taylor & Francis
Taylor & Francis Group

Check for updates

Correlative polarizing light and scanning electron microscopy for the assessment of talc in pelvic region lymph nodes

Sandra A. McDonald[a], Yuwei Fan[a,b,c], William R. Welch[d], Daniel W. Cramer[e], Rebecca C. Stearns[b], Liam Sheedy[a], Marshall Katler[b], and John J. Godleski[f,g,h]

[a]John J. Godleski, MD PLLC, Milton, MA, USA; [b]Electron Microscopy Laboratory, Department of Environmental Health, Harvard TH Chan School of Public Health, Boston, MA, USA; [c]School of Dental Medicine, Boston University, Boston, MA, USA; [d]Department of Pathology, Brigham and Women's Hospital, Boston, MA, USA; [e]Obstetrics and Gynecology Epidemiology Center, Brigham and Women's Hospital, Boston, MA, USA; [f]John J. Godleski, MD PLLC, Milton, MA, USA; [g]Harvard Medical School, Pathology Emeritus, Boston, MA, USA; [h]Department of Environmental Health at Harvard TH Chan School of Public Health, Boston, MA, USA

ABSTRACT

Perineal talc use is associated with ovarian carcinoma in many case-control studies. Such talc may migrate to pelvic organs and regional lymph nodes, with both clinical and legal significance. Our goal was to differentiate talc in pelvic lymph nodes due to exposure, versus contamination with talc in the laboratory. We studied 22 lymph nodes from ovarian tumor patients, some of which had documented talc exposure, to quantify talc using digestion of tissue taken from paraffin blocks and scanning electron microscopy/energy dispersive X-ray analysis (SEM/EDX). Talc particles correlated significantly with surface contamination assessments using polarized light microscopy. After adjusting for surface contamination, talc burdens in nodes correlated strongly with perineal talc use. In a separate group of lymph nodes, birefringent particles within the same plane of focus as the tissues in histological sections were highly correlated with talc particles within the tissue by *in situ* SEM/EDX (r = 0.80; p < 0.0001). We conclude that since talc can be a surface contaminant from tissue collection/preparation, digestion measurements may be influenced by contamination. Instead, because they preserve anatomic landmarks and permit identification of particles in cells and tissues, polarized light microscopy and *in situ* SEM/EDX are recommended to assess talc in lymph nodes.

Introduction

In diseases related to foreign particulate exposure, accurate quantification of foreign material in tissue is important to document exposure and to correlate with disease occurrence or severity related to that tissue.[1] The issue is perhaps best appreciated for asbestos and pulmonary mesothelioma and fibrosis.[2] The most comprehensive quantification is obtained by digestion of a tissue sample, which uses much larger amounts of tissue that can be assessed in a histologic tissue section.[1] The procedure can be used to identify and quantify individual fibers by transmission electron microscopy (TEM) or scanning electron microscopy (SEM) and characterize them by energy dispersive x-ray analysis (EDX) to verify that their elemental signatures are compatible with a specific type of asbestos or other foreign material exposure[3] Application of TEM and/or SEM and EDX to tissue sections cut from paraffin blocks also provides quantification when the concentration of particles in tissue is sufficiently high.[4,5] This procedure may also show where the foreign material resides within a tissue section, such as exogenous particles localizing in macrophages within lymph nodes.[6] An estimate of foreign particulate exposure may also be obtained by studying histologic tissue sections under polarized light microscopy, which highlights birefringent material and its size and shape.[7,8] Besides the use of these methods in scientific studies to characterize exposures and disease, these techniques have also been used in medicolegal contexts related to claims of injury from various exposures, including asbestos.[1]

CONTACT Sandra A. McDonald ✉ sandram8690@gmail.com ⊙ John J. Godleski MD PLLC, 304 Central Ave., Milton, MA 02186; 175Q Centre Street, Quincy, MA 02169

Color versions of one or more of the figures in the article can be found online at www.tandfonline.com/IUSP.
Supplemental data for this article can be accessed here.

One exposure of great current medical, public health, and medicolegal importance is the association of ovarian cancers with the use of talc cosmetic products in the genital area. Data related to this association come from epidemiologic studies which identified a clear excess of women with ovarian malignancy who had used talc in their genital area prior to developing cancer, compared to control women.[9–13] The International Agency for Research on Cancer has declared the use of talc (not containing asbestos) in the genital area as possibly carcinogenic (Class 2B) (IARC monograph, 2010).[14] The most recent summary of the epidemiologic data in 2018 found that genital talc use may increase the risk for ovarian carcinoma by about 30%.[15] Although the origin of the hypothesis about talc and ovarian cancer came, in part, from description of talc in ovarian tissue,[16] demonstration that talc is present in the ovarian tissue or the genital tract from women with ovarian cancer has not been a component of the epidemiologic studies, and published data regarding talc in women's pelvic organs is very limited. A study by Heller et al.[17] was done with digestion techniques followed by TEM on ovaries from 24 women having hysterectomy/oophorectomy for reasons other than ovarian malignancy. This study found talc in approximately half the samples, with no obvious correlation with genital talc use history, thereby suggesting to the authors that talc exposure may be relatively ubiquitous across the population. A subset of authors from the present study have previously described a case report[6] in which a woman with serous carcinoma of the ovary, and a history of talc usage in her genital area, was demonstrated to have talc in three of four examined pelvic lymph nodes.

In the study reported here, we assessed talc in a sizable set of lymph nodes of the pelvic region, representing multiple patients. Thus, we expanded on the lymph node analysis in the previous case report[6] as well as the study of non-malignant ovaries by Heller et al.[17] and we examined nodes in 22 patients with various types of ovarian tumors. We included the additional step of an independent polarized light microscopy study on the histological sections for each case; this procedure assessed the quantity and location of birefringent particles in relationship to tissue landmarks.

By digesting the lymph node samples, assessing the presence of talc by SEM/EDX, and comparing that data to the findings by light microscopy, we assessed tissue surface contamination as a factor explaining the high talc burden in some cases, as opposed to talc that migrated to the nodes from perineal exposure. We also endeavored, by studying a separate group of lymph node cases, to show that polarized light microscopy is a useful adjunct to *in situ* SEM/EDX, since both preserve anatomic landmarks and can serve as indicators of talc whose source is not due to contamination.

Materials and methods

Twenty-two women with ovarian tumors who had received their care in 2004 and 2005 at the Brigham and Women's Hospital (BWH), and who had participated in larger epidemiologic studies of ovarian cancer in Eastern Massachusetts and New Hampshire, were selected for the study. Women in this series were selected consecutively on the basis of meeting eligibility criteria and not on the basis of whether they had used talc. To be eligible, cases must have had lymph nodes removed from the pelvic region as part of their surgery. Cases were ineligible if the only nodes available contained metastatic disease or if there was only one unaffected node available. Though most of the cases were malignant ovarian neoplasms, two cases (one a borderline tumor and the second a granulosa cell tumor) were included because the study's objective was focused on the quantification of talc in tissue and understanding contamination vs. exposure related findings. Relevant clinical data were available both from the medical record and questionnaires completed by the women that included information on the use of talc in the genital area or as a body powder. The study was approved by the BWH Institutional Review Board and the informed consent signed by the women included permission to study material removed at the time of surgery. This group of women had both digestion studies and light microscopic studies of their lymph nodes. For our purposes, nodes of interest included inguinal, iliac, and paraaortic, and potentially any node of the pelvic region used for sampling and/or staging in ovarian surgical oncology. In some cases, the

designation "pelvic lymph node" with laterality, but without further anatomic specification, was provided with a sample.

Talc is readily visible under polarizing light microscopy, where it may be found as both plates and fibrous forms, and where the particles or fibers are brightly birefringent and often in the size range 1–10 μm. Identification of talc by electron microscopy and energy-dispersive X-ray analysis (EDX), includes the plate-like particulate or fiber-like structure and a spectrum showing magnesium and silicon peaks within 5% of the theoretical atomic ratio of 0.75 and atomic weight percent ratio of 0.649.

For each patient case, we ascertained that an acceptable representative hematoxylin-eosin (H&E)-stained slide was available for the block prior to subsequent steps. Tissue was totally cut from the paraffin block with a cleaned scalpel, heat deparaffinized, and then multiple extractions were done with xylene to remove all residual paraffin. The tissue was weighed, then added to glass centrifuge tubes, and sodium hypochlorite solution was added for digestion over a 24–48 hr period. When digestion was complete, samples were centrifuged and the sediment resuspended in filtered distilled water and vortexed until no sediment was visible. The tubes were centrifuged again and the supernatant aspirated. Sediments were resuspended in 25% ethanol, mixed by vortexing and filtered through a 13 mm, 0.2 μm Millipore filter. Tubes were washed twice with 25% ethanol and filtered. Filters were dried in a desiccator and were mounted on a carbon planchette.

Samples were analyzed in a scanning electron microscope (Leo 1460VP) equipped with an EDX spectrometer (Oxford instruments with Inca software) or an Hitachi SU6600 field emission scanning electron microscope with Oxford EDX (Xmax 50SDD EDX detector) and Oxford instrumentation software (Aztec 3.3). At 2000x magnification, 200 particles or 100 random fields were analyzed for each case, whichever came first. Using various parameters, including the number of talc particles identified by their chemical composition, the area of each microscopic field times the number of fields examined, and the overall filter area, an estimate for the total number of talc particles in the specimen was calculated.

Because fat, fibrous tissue, and lymph node contributed to the weight of the material used for digestion and because there were differences in birefringent particle distribution patterns of the tissue surface, fat and fibrous tissue, and lymph node, a more accurate approach was needed by which we could estimate the contributions of the separate locations. Tissues on all slides were digitized. Using NIH Image J analysis software (an open source image processing program, www.imagej.com), the total areas (cm^2) of the tissue on the slides for each case were calculated, as well as the respective components of lymph node and fibroadipose (soft) tissue, with the sum of these areas adding up to the total tissue area. These figures were then multiplied by 0.25 cm (a typical thickness for tissue in paraffin cassettes from which the digested tissues were derived) to obtain total specimen volumes for the total tissue, and for the lymph node and soft tissue components. The total number of talc particles identified in the digestate by SEM was then divided by the total tissue volume to obtain the number of talc particles per unit volume (cm^3).

H&E slides of intact lymph node tissue corresponding to each digested paraffin sample were analyzed with an Olympus BH-2 light microscope equipped with polarizing filter capabilities (analyzer and rotating polarizer with specimen slide in between). Each slide was scanned systematically and completely at 200x magnification under polarized light. Slides typically contained one to several lymph node profiles with adherent fibroadipose tissue. Birefringent particles visually consistent with talc (typically 1–10 μm with birefringence) were counted that were located within the lymph node parenchyma and sinuses, and a separate count was made of particles in fibroadipose (soft) tissue, i.e. not within the lymph nodes proper. The counts of these two components were added to get the total count. Particles within fibroadipose tissue were counted only if they were at least one 400x (high-power) field away from the surface, so that obvious surface contamination was not included in the counts. The birefringent particles present within lymph nodes were taken to indicate clinically significant talc that migrated there through the lymphatic system. Birefringent particles on the physical surface of the tissues were not counted for these analyses but instead assessed as described below.

Using the aforementioned image analysis data which provided the areas (cm^2) for the total tissue on the slide as well as the lymph node and soft tissue components, for each slide, the respective tissue volumes were calculated by multiplying the areas by 4 μm (4×10^{-4} cm), a standard tissue section thickness on glass slides. The number of birefringent particles per unit volume were then calculated (through simple division) for each tissue component and for the overall tissue. This meant that the volume correction factor between tissue blocks and tissue slides was approximately 625 (0.25 cm thickness of tissue in blocks vs. 4 μm thickness of slides).
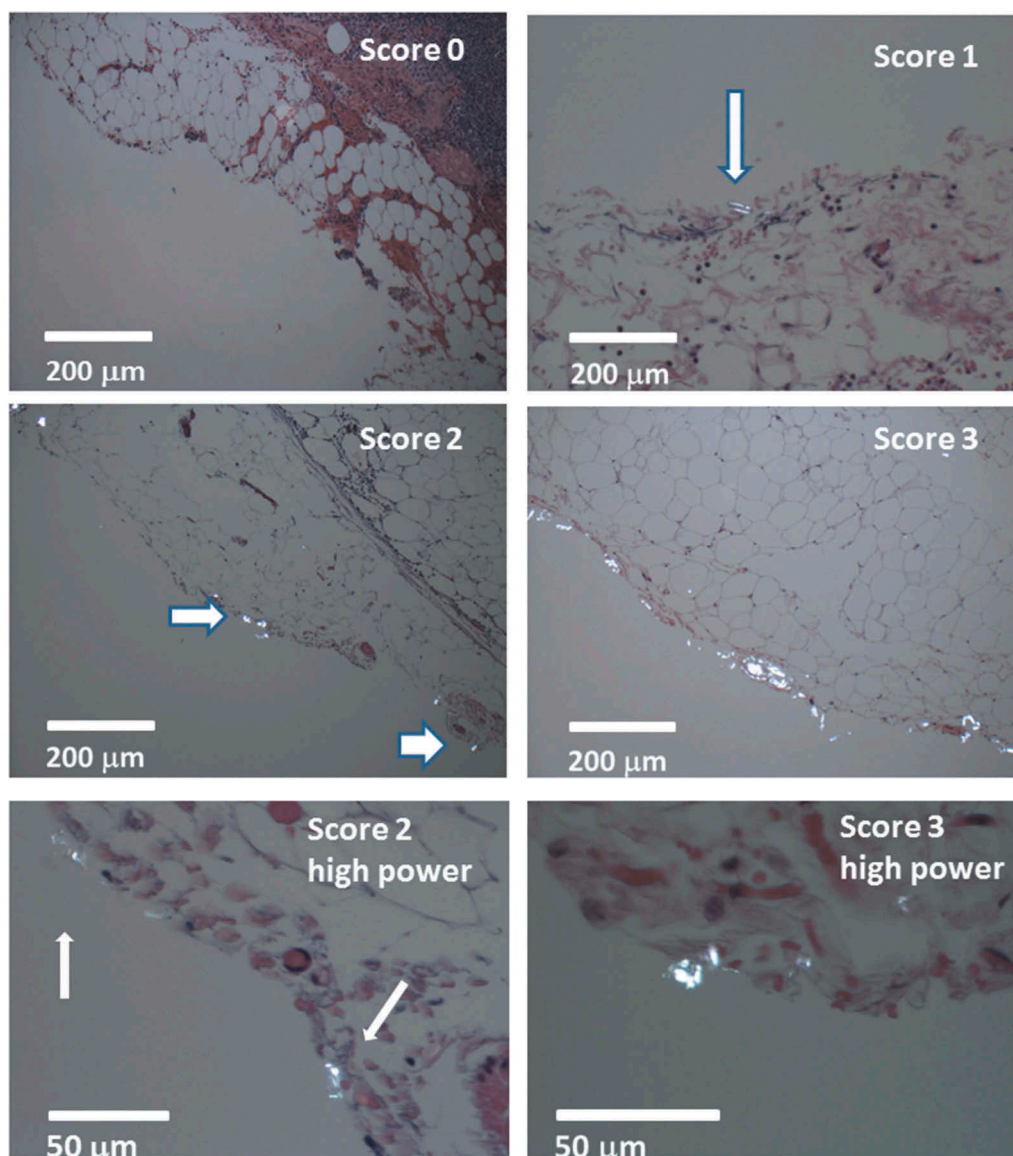
Additionally, for each of the 22 cases, a semi-quantitative visual estimate of surface contamination was made. This was done by observing the quantity and pattern of all polarizable material (typically birefringent particles of 1–10 μm, plus larger material such as paper, organic fibers, and other debris) that were present along the specimen edge and/or within one 400x (high power microscopic field) width from it. The objective here was to measure the degree to which the specimen surfaces might have been contaminated by physical manipulation during the acquisition and handling steps of the specimen in the Pathology department. Our estimate scores ranged from 0 to 3 and the criteria for the scoring was as follows (see Figure 1): 0, no polarizable material along surface; 1, occasional foreign particulates, rarely forming small clusters; 2, moderate numbers of surface particulates, forming occasional clusters or surface patches more numerous than in score 1; 3, frequent patches of particulates along with confluent stretches of contamination along the surface. Typically, such contamination was seen along the fibroadipose tissue surface with the nodal tissue interior to that. The contamination consisted typically of a mix of larger debris consistent with paper, along with smaller birefringent particulates similar to those seen and described in tissue sections (Figure 1). All contamination scores were done by a pathologist (JJG) in a blinded fashion (SEM and clinical data were unavailable at the time of scoring). A randomly chosen subset of the same cases was independently scored by a second pathologist (SM), also in a blinded fashion, to confirm successfully that the review

standards agreed, and thus the scoring standards were being applied consistently.

Subsequent statistical analysis for the 22 cases was handled as follows: Talc counts were log transformed to create normal distributions. Spearman correlations were calculated to assess the relationship between potential contamination on the talc counts and each continuous variable, and partial correlations were used to examine the relationships between talc counts, adjusted for contamination. Linear regression was used to calculate crude and contamination-adjusted talc/total volume geometric means and 95% confidence intervals.

Also, as part of this report, we studied a second group of 19 lymph node specimens from 10 ovarian carcinoma cases. The 10 cases were consults of authors JJG and WW, which were de-identified, i.e. reported here without any patient identifiers, including the 18 recognized HIPAA identifiers.[18] All 19 tissue specimens had histologic slides and corresponding paraffin blocks available. In this component of the study, we assessed the relationship of the numbers of birefringent particles in the lymph node parenchyma in histological sections, and talc particles found by *in situ* SEM/EDX at deeper levels in the tissue blocks corresponding to those sections. Digestion was not performed on these cases; nor was information available on their talc exposure. Birefringent particles in the lymph nodes were exhaustively quantified by light microscopy as previously described (particles counted in respective lymph node and soft tissue components, added to a total count for each slide). The histologic slides typically contained from one to several lymph node profiles, each with adherent fibroadipose tissue. Counting was done without regard to the number of profiles; i.e. an aggregate count was obtained across all lymph node tissue on a slide.

The tissue blocks were handled with a procedure for *in situ* SEM/EDX distinct from the tissue digestion and filter analysis by SEM described in the previous component of the study. This *in situ* procedure was first described by Thakral and Abraham[4] for assessment of particulate materials in paraffin-embedded tissue. In the study reported here, the blocks were handled with particle-free gloves on pre-cleaned surfaces and sectioned removing ~30 micrometers of tissue

Figure 1. Tissue surface contamination score semi-quantitative grading. As shown especially in the two high-power images at bottom, the contamination material consisted typically of larger debris consistent with paper, along with smaller birefringent particulates. Surface contamination was typically found along the fibroadipose tissue surface, with lymph node tissue located underneath. Grading scheme is as follows: **Score 0**: no polarizable material along surface. **Score 1**: occasional birefringent particulates (arrows), rarely forming small clusters. **Score 2**: moderate numbers of surface birefringent particulates (arrows), forming occasional clusters or surface patches more numerous than in score 1. **Score 3**: frequent patches of particulates along with confluent stretches of contamination along the surface. (All images under polarizing light microscopy, H&E staining, all 100x except 400x [original magnification] in the bottom two images which respectively show score 2 and 3).

and paraffin using a rotary microtome with a new, clean stainless-steel blade. This sectioning was intended to remove any surface contamination from previous storage and handling. After the fresh surface was exposed, the block surfaces were washed in distilled, deionized water for 30 seconds to remove soluble surface materials such as sodium chloride and sodium phosphates used in processing for histology. The blocks were mounted for SEM examination and always kept in closed containers to limit any lab contamination. These tissue surfaces were studied with a Hitachi SU6600 field emission SEM with an Oxford EDX with Aztec version 2.0 to 3.3 software, and EDX detector model X-Max 50 SDD. The backscatter mode of the microscope highlighted mineral particles within the tissues. Areas of the tissue at the sectioned block surface were

examined at relatively low magnification 200-500x, and when particles were seen, they were then examined at higher magnification for morphological characteristics and to carry out spectral analysis on each particle found. Electron beam penetration depth under the conditions used was estimated to be 2.5 μm, with an analysis range of 0.5–2.5 μm. Of note, under *in situ* SEM the interior tissue and exterior tissue surfaces were readily distinguishable; this distinction was important for our study. In particular, as subsequent discussion will show, it was important to avoid analyzing surface particulates and instead analyze those inside the tissue. Having a scanned photocopy of the light microscopic slide and the block surface available for reference when performing SEM/EDX helped in navigating the anatomic landmarks, including surface vs. tissue interior location. We subsequently carried out an auxiliary part of this study, in which surface contamination of tissue slides was assessed using two of the cases that had this finding. The surface particles were assessed by *in situ* SEM/EDX to determine the identity (i.e. chemical composition) of the surface contamination.

For this second part of the study, linear regression analyses, with the generation of a coefficient of determination (r) goodness-of-fit value, were done between three statistical pairings: total birefringent particles by light microscopy vs. *in situ* SEM/EDX talc counts, lymph node birefringent particles vs. *in situ* SEM/EDX talc count, and fibroadipose tissue birefringent particles vs. *in situ* SEM/EDX talc counts. Our hypothesis was that the first two pairings would be correlated but the last one would not. The inclusion of multiple specimens from some of the patients meant that the 19 data points (specimens) were not truly independent of each other from the perspective of the population. However, from a statistical point of view, this was justified because, in this phase of our study, the purpose was an evaluation of methods and data related to the samples themselves, and not the population from which the samples were drawn.

Results

Digestion study

Table 1 shows characteristics of the 22 subjects enrolled in the BWH node digestion study, arrayed (least to greatest) by the amount of talc (by digestion) per cm^3 tissue volume. Fourteen (64%) of the women had invasive serous ovarian carcinoma of the ovary, which in one case was mixed with endometrioid carcinoma. Nineteen of the 22 nodes (86%) were external iliac, with 11/19 (58%) from the right side. The age range of the women was 38–73 with a median of 56; 10 (45%) had used talc in their genital area and 16 (73%) had used it as a body powder. There was considerable variation in total talc counts seen after digestion of the nodes. There was also considerable variation in birefringent particle counts in the nodal components, as well as corresponding counts per cm^3 tissue volume (see column totals where pertinent). The number and proportion of nodes with 0, 1, 2, and 3 surface contamination scores were: 4(18%), 7(32%), 7(32%), and 4 (18%).

Of note, cases 4, 9, and 13 had no clinical exposure history, and yet all had high contamination scores (either 2 or 3) and corresponding moderate to high talc counts per cm^3 tissue volume, thus highlighting a role for contamination in their digestion results. In contrast, cases 10 and 18 had clinical **exposure, but** zero contamination scores (i.e. no visible surface contamination); they also had significant talc counts per cm^3 tissue volume, indicating that in the absence of surface contamination, clinical exposure yields significant talc counts using digestion. Case 18 can also be contrasted with cases 19–22, which had the four highest talc counts per cm^3 tissue volume (Table 1), and all of which had high levels of surface contamination.

Table 2 shows Pearson and partial correlations among the various quantitative measurements related to talc and birefringent particles. The degree of surface contamination (0–3 score) as it correlates with other measures of talc and birefringent particles within the node is shown in the right-most column. The surface contamination score was significantly correlated with: the total talc particle count by digestion (r = 0.43, p = 0.05); with birefringent particle counts by light microscopy in the soft tissue (fibroadipose) component (r = 0.53, p = 0.01); with total talc per cm^3 tissue volume by SEM/EDX (r = 0.57, p = 0.006); and with birefringent particle counts in fibroadipose tissue per cm^3 fibroadipose volume (r = 0.51, p = 0.01). The remainder of correlations and p values in Table 2 represent those for partial correlations

Table 1. Clinical data and talc digestion and light microscopic data among the first patient group (BWH cases).

Case number	Tumor histology	Node*	Component volume (cm³) Total	Node	Fat	Age	Talc use Genital	Body	Total talc †	Talc/cm³ of tissue volume	Total birefringence counts†† Total	Node	Fat	Birefringence per component volume (particles/cm³) Total	Node	Fat	Surface contamination
1	Endometrioid	REI	0.341	0.195 (57%)	0.146 (43%)	60	No	Yes	844	2,475	3750	1250	2500	11,000	6,375	17,250	1
2	Serous invasive	LP	0.334	0.171 (51%)	0.164 (49%)	53	No	Yes	1608	4,800	1250	625	625	3,737	3,661	3,812	1
3	Serous invasive	LEI	0.308	0.119 (39%)	0.188 (61%)	69	No	Yes	2065	6,705	10625	6250	4375	34,552	52,301	23,271	0
4	Serous invasive	LEI	0.407	0.252 (62%)	0.155 (38%)	38	No	No	4290	10,540	4375	1250	3125	11,187	4,960	20,187	2
5	Clear cell	REI	0.332	0.189 (57%)	0.143 (43%)	54	No	Yes	3965	11,942	15000	12500	2500	45,146	66,286	17,406	0
6	Serous invasive	REI	0.232	0.169 (73%)	0.063 (27%)	50	Yes	No	3378	14,500	1250	625	625	5,387	3,687	9,937	1
7	Endometrioid	REI	0.557	0.392 (70%)	0.165 (30%)	46	No	No	8920	16,000	4375	1250	3125	7,912	3,187	18,937	1
8	Serous invasive	LEI	0.107	0.039 (36%)	0.069 (64%)	49	Yes	Yes	2533	23,562	1250	0	1250	11,687	0	18,375	1
9	Endometrioid	REI	0.533	0.089 (17%)	0.444 (83%)	57	No	No	19,094	35,823	15000	3125	11875	28,103	35,014	26,715	2
10	Granulosa cell	REI	0.237	0.206 (87%)	0.030 (13%)	49	Yes	Yes	20,267	85,600	4,375	3,125	1,250	18,500	15,125	41,375	0
11	Serous invasive	REI	0.107	0.092 (86%)	0.015 (14%)	51	No	No	10,390	97,100	5,000	625	4,375	46,750	6,812	291,687	2
12	Serous invasive	RP	0.026	0.021 (79%)	0.006 (21%)	51	Yes	Yes	2,834	107,300	10,625	5,625	5,000	402,437	269,125	908,750	2
13	Serous invasive	LEI	0.147	0.022 (15%)	0.125 (85%)	68	No	No	16,057	115,030	16,875	1,250	15,625	114,812	56,562	125,125	3
14	Serous invasive	REI	0.219	0.145 (66%)	0.074 (34%)	73	Yes	Yes	30,330	138,500	8,125	1,875	6,250	37,062	12,937	84,437	2
15	Endometrioid	REI	0.506	0.083 (16%)	0.423 (84%)	58	Yes	Yes	73,267	144,800	26,875	12,500	14,375	53,125	151,500	33,937	2
16	Serous borderline	REI	0.147	0.055 (37%)	0.092 (63%)	60	No	Yes	21,409	145,600	11,875	2,500	9,375	80,812	45,437	101,875	1
17	Serous invasive	LEI	0.174	0.123 (71%)	0.051 (29%)	62	Yes	Yes	33,778	194,100	30,625	28,125	2,500	176,000	228,687	49,437	1
18	Serous invasive	LEI	0.323	0.203 (63%)	0.121 (37%)	53	Yes	Yes	67,557	208,200	>125,000	>125,000	625	>387,000	>616,365	3,000	0
19	Serous invasive	LEI	0.052	0.017 (33%)	0.035 (67%)	69	No	Yes	12,661	242,100	11,250	1,250	10,000	215,000	71,875	285,625	3
20	Serous invasive	LEI	0.286	0.185 (65%)	0.101 (35%)	66	Yes	Yes	92,891	325,200	4,375	3,125	1,250	15,312	16,875	12,437	2
21	Endometrioid	REI	0.056	0.039 (70%)	0.017 (30%)	51	No	Yes	85,041	1,518,589	13,750	1,250	12,500	246,875	32,051	735,294	3
22	Serous/ endometrioid	RPA	0.424	0.284 (67%)	0.139 (33%)	69	Yes	Yes	797,171	1,881,500	>62,500	>62,500	1,250	>147,500	>220,062	9,000	3
Median			0.262	0.134	0.111	56			14,359	102,200	10,625	2,188	3,125	41,104	33,533	24,993	

*Location of Node: LEI = Left external iliac; REI = Right external iliac; RPA = Right paraaortic; LP = Left pelvic; RP = Right pelvic
†Total number of talc particles by digestion (calculated)
††Total birefringence counts = particles in field x 625 (see Materials and Methods)
Node refers to lymph node parenchyma areas as measured by Image J software and studied by light microscopy (see Materials and Methods).
Fat refers to fibroadipose soft tissue areas as measured by Image J software and studied by light microscopy
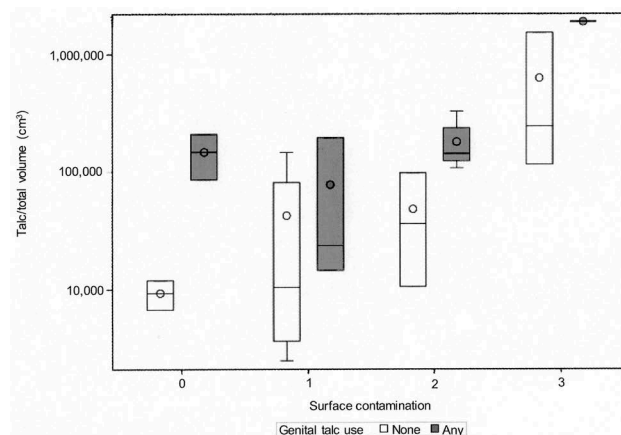
Table 2. Correlations between surface contamination, talc, and age (r and p values).

Variable*	Surface contamination r (p)	Total talc by digestion r (p)	Total birefringent particle counts Total r (p)	Node r (p)	Fat r (p)	Talc/total volume r (p)	Birefringent particle counts per cm³ volume Total r (p)	Node r (p)	Fat r (p)
Total talc by digestion	0.43 (0.05)								
Total birefringent particle counts	0.15 (0.51)	0.67 (0.001)							
Total birefringent particle counts, node	−0.07 (0.77)	0.59 (0.005)	0.81 (<.0001)	0.07 (0.76)					
Total birefringent particle counts, fat	0.53 (0.01)	−0.13 (0.58)	0.25 (0.26)	0.47 (0.03)	−0.06 (0.78)				
Talc/cm³ volume	0.57 (0.006)	0.87 (<.0001)	0.63 (0.002)	0.56 (0.008)	0.3 (0.19)	0.68 (0.0007)			
Birefringent particles per cm³ total volume	0.33 (0.13)	0.42 (0.06)	0.82 (<.0001)	0.88 (<.0001)	0.18 (0.45)	0.64 (0.003)	0.87 (<.0001)		
Birefringence per cm³ node volume	0.07 (0.77)	0.51 (0.02)	0.90 (<.0001)	0.88 (<.0001)	0.61 (0.003)	0.16 (0.48)	0.45 (0.04)	0.13 (0.58)	
Birefringence per cm³ fat volume	0.51 (0.01)	−0.24 (0.30)	0.003 (0.99)	−0.1 (0.68)	0.16 (0.49)	0.22 (0.33)	0.26 (0.25)	0.36 (0.12)	−0.07 (0.75)
Age	0.28 (0.20)	0.26 (0.26)	0.35 (0.12)	0.32 (0.15)					

Node = lymph node tissue
Fat = fibroadipose tissue

adjusted for the level of surface contamination. Not unexpectedly, total counts always strongly correlated with counts per cm³ of relevant tissues: e.g. total talc with total talc per cm³ tissue volume (r = 0.87, p = 0.001); total birefringent particle counts in lymph node tissue with birefringent counts per cm³ lymph node tissue (r = 0.88, p = 0.0001); and birefringent particle counts in fibroadipose tissue with birefringence counts per cm³ fibroadipose volume (r = 0.61, p = 0.003). Talc counts per cm³ tissue volume correlated with: birefringent particles per cm³ tissue volume (r = 0.68, p = 0.007), and lymph node birefringent particles per cm³ lymph node tissue (r = 0.64, p = 0.003), but not with fibroadipose birefringent particles per cm³ fibroadipose tissue. Total birefringent particles per cm³ tissue volume correlated best with lymph node birefringent particles per cm³ lymph node tissue (r = 0.89, p = 0.001). Birefringent particle counts per cm³ lymph node tissue were not correlated with fibroadipose birefringent particle counts per cm³ fibroadipose volume. Age was not significantly correlated with any measure of nodal contamination.

Figure 2 and Table 3 illustrates the potential effect of surface contamination on the interpretation of the relationship between total talc (by digestion) per cm³ tissue volume. Figure 2 illustrates that for any level of surface contamination, those who used talc in the genital area had a higher amount of talc than those who had not used talc genitally. Table 3 quantifies

Figure 2. Talc/total volume for genital talc users and non-users by surface contamination This figure shows surface contamination scores (x axis) plotted against talc per tissue volume (y-axis, logarithmic scale), showing that for any level of surface contamination, those who used talc in the genital area had a higher amount of talc than those who had not used talc genitally.

Table 3. Geometric mean talc/total volume by genital talc use.

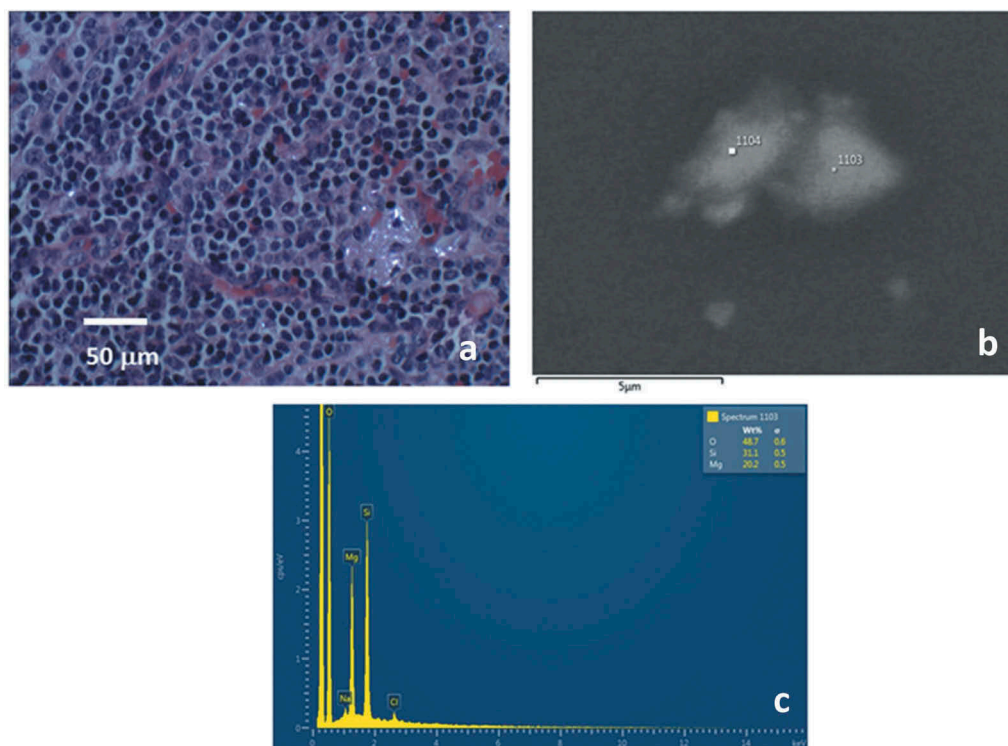| Talc/total volume	No genital talc use (n = 12) Geometric mean (95% CI)	Any genital talc use (n = 10) Geometric mean (95% CI)	p-value
Crude	35,049 (13,637, 90,079)	131,584 (46,787, 370,070)	0.08
Adjusted for surface contamination	29,926 (15,546, 57,605)	159,056 (77,491, 326,475)	0.004

this effect more precisely and indicates that, overall, the genital talc user had higher talc counts per volume of tissue than those who had not used talc, but the association was of borderline significance. After adjustment for level of surface contamination, the association became significant (p = 0.004) with the level of talc in nodal tissue at least five times higher in those who used talc genitally compared to those who had not.

Figure 3 shows correlative polarizing light microscopy, SEM, and EDX from case 18 in the digestate study (Table 1). Going clockwise from upper left, panel **A** shows polarized light microscopy (H&E, 200x), showing numerous birefringent particles (general size range 1 to 5 μm) within the macrophages of

a left external iliac lymph node. This case was near the upper end of the range of particle abundances we observed. Panel **B** shows examples of two particles (labeled 1103 and 1104), identified by SEM on the digestate filter, each <5 μm diameter. Panel **C** shows the spectrum for particle 1103, with an Mg-Si atomic weight ratio of 0.6495, characteristic of talc. The other particle in **B**, 1104, had an Mg-Si ratio within 5% of the theoretical talc value (0.649).

In situ *SEM study*

Table 4 shows data for the second part of the study (19 lymph node specimens from 10 patients). The left-most two columns (case number and block letter) are

Figure 3. Correlative polarizing light microscopy, SEM, and EDX from case 18 in the digestate study (Table 1). Clockwise from upper left: **a**, Polarizing light microscopy, H&E, 200x, showing numerous birefringent particles (general size range 1 to 5 μm) within the macrophages of a left eternal iliac lymph node. **b**, Two particles (labeled 1103 and 1104), identified by SEM on the digestate filter, each <5 μm diameter. **c**, Spectrum for particle 1103, The Mg-Si atomic weight ratio is 0.6495, characteristic of talc. The other particle in **b**, 1104, had an Mg-Si atomic weight ratio within 5% of the theoretical talc value (0.649).

Table 4. Correlation between light microscopic birefringent particulates and in situ SEM analysis for talc particles.

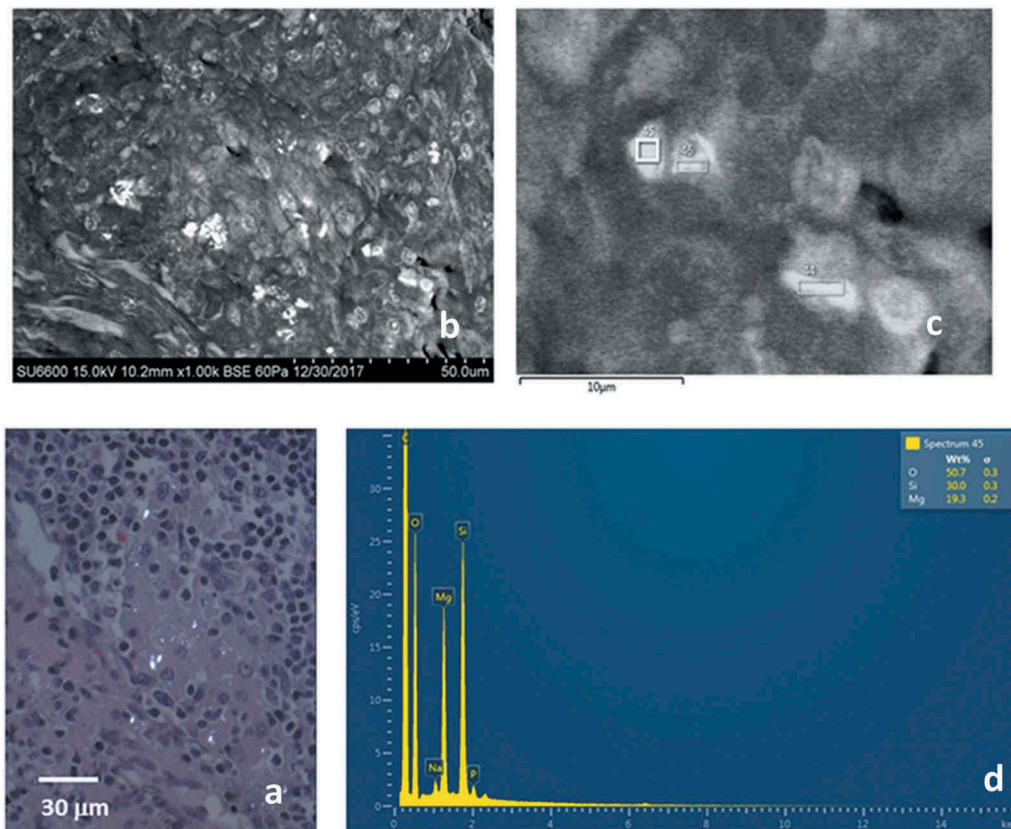| Case number	Slide letter	Birefringent particles in lymph node tissue (total per slide)	Birefringent particles in surrounding fibroadipose tissue (total per slide)	Total birefringent particles in slide (columns C + D)	Number of talc particles in the block by in situ SEM
1	A	3	5	8	0
	B	55	7	62	5
2	A	5	2	7	9
3	A	2	0	2	0
	B	0	0	0	0
4	A	19	9	28	31
	B	3	1	4	5
5	A	>500	3	>500	65
6	A	6	4	10	0
	B	8	3	11	0
	C	16	4	20	0
7	A	7	3	10	1
	B	1	0	1	0
8	A	>100	3	>100	18
	B	>200	2	>200	43
	C	>100	5	>100	35
	D	>100	7	>100	24
9	A	8	6	14	1
10	A	15	>50	>50	12

In this part of the study, 19 pelvic lymph node slides on 10 ovarian carcinoma patients (with each patient having from one to four node specimens), showed the relationship of the numbers of birefringent particles (by light microscopy) within histological sections (separately categorized in lymph node and fibroadipose tissue components), and talc particles found by SEM/EDX at deeper levels in the tissue blocks corresponding to those sections (right-hand column). In case 9C, the vast majority of the birefringent particles were localized in only one of several lymph nodes visible in the slide. Note that cases with very numerous particle counts by light microscopy are designated simply as greater than a certain threshold.

fully de-identified and serve for identification purposes within the table only. The table shows the relationship of the numbers of birefringent particles by light microscopy within histological sections (separately categorized in lymph node and fibroadipose tissue components), and talc particles found by SEM/EDX on the block surface (following the preparation procedure) corresponding to those sections (right-most column). Consistent with our hypotheses, strong correlations using Spearman correlations were indeed evident between a) lymph node counts by light microscopy and the SEM total talc count ($r = 0.80$, $p < 0.0001$); and b) total particle counts by light microscopy and the SEM total talc count ($r = 0.79$, $p < 0.0001$). Fibroadipose tissue counts by light microscopy did not correlate with SEM total talc counts ($r = 0.32$, $p =$ not significant). In controlling for correlated observations from the same patient,

Spearman correlations using one record per case were done for the six patients where more than one lymph node specimen was included in the study (among these patients, the specimen with the highest SEM talc count was the one selected). With this adjustment, strong correlations were still observed using Spearman correlations as evident between a) lymph node counts by light microscopy and the SEM total talc count ($r = 0.69$, $p < 0.03$); and b) total particle counts by light microscopy and the SEM total talc count ($r = 0.74$, $p < 0.01$), Fibroadipose tissue counts by light microscopy did not correlate with SEM total talc counts ($r = 0.16$, $p =$ not significant).

Figure 4 shows correlative polarizing light microscopy, *in situ* SEM, and EDX on case 9C from Table 4. Going clockwise from lower left, panel **A** shows numerous birefringent particles under polarized light microscopy (H&E, 400x) within the macrophages of a left external iliac lymph node. Panel **B** shows low-power backscattered electron imaging under SEM with several positive particles. Panel **C** shows an enlarged (cropped) view of the lower right-hand part of panel B. Three particles are labeled – 44, 45, and 46. Panel **D** shows the spectrum for particle 45, which showed an Mg-Si ratio of 0.643. Particle 44 was also within the 5% of the theoretical value of 0.649 and so was considered talc as well. Particle 46 had an Mg-Si ratio of 0.610, which falls just outside the 0.649 ± 5% range for talc, and so it was considered a nonspecific magnesium silicate.

A review of the non-talc particles found by *in situ* SEM in the 10 patients in Table 4 showed an aggregated total of 310, which based on their chemical composition would be regarded as likely birefringent. Of these, the most common were magnesium silicates outside the 5% theoretical range of the Mg-Si atomic weight spectral ratio for talc (113 total particles or 36%), aluminum silicates with or without magnesium (91 total particles or 29%), and calcium without phosphate (41, or 13%), with others accounting for the remaining 22%. Non-fibrous, non-talc silicates are known to have a longer dissolution time than talc in physiologic conditions; the dissolution time for talc is approximately 8 years for a 1 μm particle.[19] Thus, the component of non-talc silicates in pelvic tissues could proportionally rise over sufficient

Figure 4. Correlative polarizing light microscopy, in situ SEM, and EDX on case 8C from Table 4. Clockwise from lower left: **a**, Numerous birefringent particles under polarized light microscopy (H&E, 400x) within the macrophages of a left external iliac lymph node. **b**, Low-power backscattered electron imaging under SEM with several positive particles. **c**, Enlarged (cropped) lower right-hand portion of **b**. Three particles are labeled – 44, 45, and 46. **d**, Spectrum for particle 45, which showed an Mg-Si atomic weight ratio of 0.643. Particle 44 was also within the 5% of the theoretical value of 0.649 and so can be considered talc as well. Particle 46 had an Mg-Si atomic weight ratio of 0.610, which falls just outside the 5% range for talc and so can be considered a nonspecific magnesium silicate.

elapsed time (years), even if the original exposure to talc was heavy.

To provide final evidence for our hypothesis that talc is an important part of specimen surface contamination, two authors (SM and JG) re-reviewed the 19 slides from the second part of the study (*in situ* SEM). The goal was to find cases in this group with surface contamination. We did not find any with a score of 3, but two cases (1B and 7A from Table 4) were chosen that, respectively, had contamination scores of 2 and 1 (with 100% agreement by pathologists SM and JG), and substantial amounts of evaluable surface area. On polarizing light microscopy, these cases showed a mixture of larger paper debris fragments and smaller (1–10 μm) birefringent particulates along the surface similar to those previously seen for many Table 1 cases., Respectively, for 1B and 7A, 13 and 5 small birefringent particulates were

found by thorough examination of their surfaces in addition to larger paper debris. SEM of the tissue surface for block 1B (35 mm^2 analysis area) showed a total of 5 talc particles, and for 7A showed 1 talc particle (50 mm^2 analysis area). Given the 2.5 μm effective section thickness (electron beam analysis depth) and these relatively small surface areas, these SEM talc particle counts are significant, and are consistent with the light microscopic review. Thus, this portion of the study directly showed that surface contamination particles were talc, whereas previously, this had only been strongly implied by the results in Table 1. (See supplementary figure S1). In addition to the talc particles, 44 other exogenous particles were found across tissue surfaces of these two cases by SEM/EDX: 27 external mineral (mainly Si in combination with Mg and/or Al), 6 non-talc Mg-Si minerals, and 11 external metal.

Discussion

The accurate identification of talc in pelvic tissues is important because it documents exposure by demonstrating the presence of talc in these tissues and provides evidence in support of the role of talc in the epidemiological association with ovarian cancer in case-control studies.[9–13,15] The overall relative risk across the various positive studies is around 1.3, and where tumor histology data have been available for review, several common sub-types (serous carcinoma, endometrioid carcinoma, and serous borderline tumors) are most frequently involved in the association.[11,13]

Talc, when applied to the perineum, is believed to migrate to the upper genital tract, passing through the open tract to the fallopian tubes and eventually reaching the ovaries.[11,16] Talc may also gain access to the lymphatic system as a means of reaching pelvic organs and lymph nodes,[20,21] similar to the route to the pulmonary nodes of talc miners.[22] Lymph nodes of the pelvic region include several anatomic sub-classifications (inguinal, iliac, and paraaortic), with the common theme that they may receive lymphatic efferents from pelvic organs such as the ovaries and perineum and/or secondarily from other lymph nodes in the area. Ovarian carcinoma, especially serous, tends to metastasize early (when just one or two nodes are involved) to paraaortic nodes.[23] Full discussions of the lymphatic drainage/anatomy of the pelvic region are available in the literature.[20,21] Lymph nodes are often sampled during gynecologic surgery for tumor staging and assessment for metastatic disease. However, additional examination of these nodes for talc, especially in settings where genital exposure is known to have occurred, would add insight as to the ability of talc to migrate and lodge within pelvic tissues.

This study supports earlier observations that talc particles, from perineal exposure, can and do migrate to pelvic lymph nodes. Material with the microscopic and spectral features of talc was clearly demonstrated within the lymph node parenchyma in most of our cases, as scattered birefringent particles in the general size range 1–10 μm. Sometimes the material was visible within nodal macrophages, lending strong credence to a lymphatic migration route. Similar particles were also found in the fibroadipose tissue adjacent to lymph nodes, where they may have arrived via the lymphatic system, but more likely resulted from visibly present surface contamination pushed into the underlying fibroadipose tissue.

Our study took the additional critical step of comparing the light microscopic data to SEM digestion data, thereby going beyond the earlier study by Heller et al.[17] in scope, in addition to examining lymph nodes rather than ovaries. Like that earlier paper, we found high talc particle burdens in some digested samples. But because these correlated with contamination scores, we believe that the digestion counts are not fully reflective of clinically relevant talc exposure or its migration in the tissues. Instead, they are influenced by contamination, such as talc introduced by non-surgical gloves used for handling tissue and in the general lab environment during tissue collection and processing in the pathology laboratory. Thus, tissue digestion should not be regarded as a reliable quantification method for talc or contaminants of talc, especially where the collection and processing steps have not been rigidly controlled from the start. The correlation of contamination scores with counts of birefringent particles in fibroadipose tissue suggests that particles adherent to the surface (through contamination) may be pushed into the soft fibroadipose tissue, since it is typically the most peripheral type of tissue, with the nodal tissue usually deeper and encapsulated with a fibrous tissue capsule. The highly variable talc burdens found by digestive analysis and SEM, spanning approximately three orders of magnitude, are consistent with contamination influence, since the latter would be expected to vary considerably between procurement environments. However, this could also be observed in the range of burdens seen in a clinically exposed population with appropriate lab procedures/controls (Table 4).

Even though contamination played a role in total tissue counts, it was still the case that high talc burdens in the lymph nodes, when present, contributed to the SEM digestate results, hence producing the observed correlation between the two. Thus, it is likely that both contamination and clinically significant lymph node talc are reflected in the SEM digestate data. The main

problem in using digestion is that it likely raises the baseline for all patients and groups, thus potentially obscuring clinically significant differences, which would otherwise be observed if contamination were eliminated (as previously mentioned, Table 3 illustrates a robust demonstration of this effect).

By showing strong correlations between particle counts (polarized light microscopy) and *in situ* SEM analysis, the second part of our study demonstrated that the latter alternative is a better method of talc assessment than digestion, because the anatomic landmarks are preserved and surface contamination is not incorporated into the general talc count, as it is with tissue digestion. In combination with other parts of our study, this aspect also showed that the birefringent material in the lymph node tissue, is the clinically significant component related to talc exposure. Surface contamination can still be present, and our demonstration of talc on the surfaces of cases 1B and 7A by *in situ* SEM lent support to the conclusions from the first (digestion) part of the study.

A major strength of our study was the correlative light microscopic and SEM/EDX data for each case, with examination of anatomic locations in the former. This provided a key perspective in the evaluation of the talc burden data that a digestive study alone would not have given. In fact, this study demonstrates the broader principle that correlative histologic review is important in many areas of pathology – especially where digestion procedures are performed, and where the study of anatomic landmarks are needed to complement data from the latter. This is because the tissue is compartmentalized histologically, with different functions and significance for each component, a fact not always recognized by those who digest tissue routinely and use the resulting product completely in analyses such as Western blotting or mutational assays.[24]

Unfortunately, as part of our study, we were not able to also do *in situ* SEM/EDX on the intact tissues used for digestion in the first group of cases (22 patients). However, by showing that birefringent particles within lymph nodes were strongly correlated with the demonstration of talc inside the nodes by *in situ* SEM/EDX, the second part of our study filled that role, and thus 1)

material in lymph nodes is likely reflective of the clinical exposure, 2) in this clinical setting and given our results, a substantial proportion of this birefringent material is likely to be talc, 3) surface contamination is common, and so with *in situ* SEM, it is important to discern the anatomic landmarks, and avoid analyzing surface particulates (as shown by our direct demonstration of talc on the surfaces of cases 1B and 7A in our auxiliary study to the cases in Table 4).

In addition to talc, much other commonly found birefringent material, such as that described in the Results section for the SEM analysis, is likely nonspecific particulate material which finds its way into the perineum through general living and hygiene practices. Another important point is that seeing particles by *in situ* microscopy, both light and SEM, requires a relatively large amount of material distributed within the tissues in order to find it. As a demonstration of this principle, Roggli and Pratt[25] showed that finding one asbestos body in a tissue section was indicative of at least 100 fibers per gram of tissue. The calculations we used to estimate particles/cm^3 of tissue volume (Table 1), starting with a count of birefringent particles in tissue sections, illustrate a similar principle.

In the long-studied and debated association between talc exposure and ovarian cancer, our study provides additional evidence that talc may enter pelvic tissues and ultimately be detected and measured in regional lymph nodes, and this relationship became especially strong when clinical use data was considered and surface contamination was corrected for statistically. This adds perspective to the known migratory capabilities and overall biological role/impact of talc. For some of the more heavily exposed cases in the second part of the study, we noticed that the large majority of birefringent material was localized in a single node, among several present on a given slide. This suggested that pelvic drainage/migration pathways for talc may be very specific, and focused on one or relatively few nodes as an endpoint – perhaps consistent with the concept of sentinel nodes in oncologic surgery.[26]

Our findings also suggest that in patients with ovarian cancer, clinicians may want to make broader inquiries into the past and present use

of talc by their patients. Similarly, pathologists may wish to pay greater attention to sampled regional lymph nodes. In addition to the usual study of these nodes for metastases, they may wish to examine macrophages more closely for exogenous particles including by polarized light. A positive finding may trigger clinical inquiries about exposure where it was not previously suspected. Our findings yield important insights as to the ability of talc to migrate to nodes, and under what conditions its identification in nodes and tissues is clinically meaningful and when not.

In conclusion, talc contamination of the surface of surgical pathology specimens is common. Exposure (such as perineal application), whether known clinically or not, often results in significant deposition of talc in the tissues. Correlative light microscopy is needed to assess the possibility of lab contamination, and to determine if talc is truly present in clinically meaningful locations in lymph nodes or other tissues.

Declaration of Interest Statement

Funding

References

1. Abraham JL. Analysis of fibrous and nonfibrous particles. In: Rom WN, Markowitz SB, eds. *Environmental and Occupational Medicine*. 4th ed. Philadelphia: Lippincott Williams and Wilkins; 2006:277–297.

2. Roggli VL. Asbestos bodies and nonasbestos ferruginous bodies. In: Roggli VL, Greenberg SD, Pratt PC, eds. *Pathology of Asbestos-Associated Diseases*. Boston: Little Brown; 1992:39–75.

3. McDonald JW, Roggli VL, Churg A, et al. Microprobe analysis in pulmonary pathology. In Ingram P, Shelburne JD, Roggli VL, et al. eds. *Biomedical Applications of Microprobe Analysis*. San Diego: Academic Press; 1999:201–256.

4. Thakral C, Abraham JL. Automated scanning electron microscopy and x-ray microanalysis for in situ quantification of gadolinium deposits in skin. *J Electron Microsc*. 2007;56:181–187. doi:10.1093/jmicro/dfm020.

5. Shelburne JD, Estrada H, Hale M et al. Correlative microscopy and microprobe analysis in pathology. In: Bailey GW, ed., *Proceedings of the 47th Annual Meeting of the Electron Microscopy Society of America*, San Francisco: San Francisco Press; 1989: 900.

6. Cramer DW, Welch WR, Berkowitz RS, et al. Presence of talc in pelvic lymph nodes of a woman with ovarian cancer and long-term genital exposure to cosmetic talc. *Obstet Gynecol*. 2007;110:498–501. doi:10.1097/01.AOG.0000262902.80861.a0.

7. Wolman M. Polarized light microscopy as a diagnostic tool of pathology. *J Histochem Cytochem*. 1975;23:21–50. doi:10.1177/23.1.1090645.

8. McDonald JW, Roggli VL. Demonstration of silica particles in lung tissue by polarizing light microscopy. *Arch Pathol Lab Med*. 1995;119:242–246.

9. Cramer DW, Welch WR, Scully RE, Wojciechowski CA. Ovarian cancer and talc. *Cancer*. 1982;50:372–376.

10. Cramer DW, Lieberman RF, Ernstoff LT, et al. Genital talc exposure and risk of ovarian cancer. *Int J Cancer*. 1999;81:351–356.

11. Cramer DW, Vitonis AF, Terry KL, Welch WR, Titus LJ. The association between talc use and ovarian cancer: a retrospective case-control study in two US states. *Epidemiol*. 2016;27:334–346. doi:10.1097/EDE.0000000000000434.

12. Schildkraut JM, Abbott SE, Alberg AJ, et al. Association between body powder use and ovarian cancer: the African-American Cancer Epidemiology Study ((AACES). *Cancer Epidemiol Biomarkers Prev*. 2016;25:1411–1417. doi:10.1158/1055-9965.EPI-15-1281.

13. Terry KL, Karageorgi S, Shvetsov YB, et al. Genital powder use and risk of ovarian cancer: a pooled analysis of 8,525 cases and 9,859 controls. *Cancer Prev Res*. 2013;6:811–821. doi:10.1158/1940-6207.CAPR-13-0037.

14. IARC (International Agency for Research on Cancer). *Monograph 93-8C*. 2010:277–413. Lyon, France: World Health Organization.

15. Penninkalimpi R, Eslick GD. Perineal talc use and ovarian cancer: a systematic review and meta-analysis. *Epidemiol*. 2018;29:41–49. doi:10.1097/EDE.0000000000000745.

16. Henderson WJ, Joslin CAF, Turnbull AC, et al. Talc and carcinoma of the ovary and cervix. *J Obstet Gynaecol Br Commonw*. 1971;78:266–272.

17. Heller DS, Westhoff C, Gordon RE, Katz N. The relationship between perineal cosmetic talc usage and ovarian talc particle burden. *Am J Obstet Gynecol*. 1996;174:1507–1510.

18. https://www.atlanta.va.gov/Docs/HIPAA_Identifiers.pdf

19. Jurinski JB, Rimstidt JD. Biodurability of talc. *Am Mineralologist*. 2001;86:392–399. doi:10.2138/am-2001-0402.

20. Wolfram-Gabel R. Anatomy of the pelvic lymphatic system. *Cancer Radiotherapie*. 2013;17:549–552. doi:10.1016/j.canrad.2013.05.010.

21. Kubik S, Todury G, Ruttimann A, et al. Nomenclature of the lymph nodes of the retroperitoneum, the pelvis and the lower extremity. In: Ruttimann A, ed. *Progress in Lymphology*. Stuttgart: Georg Thieme Verlag; 1967:52–56.

22. Roggli VL, Benning TL. Asbestos bodies in pulmonary hilar lymph nodes. *Mod Pathol*. 1990;3:513–517.

23. Haller H, Mamula O, Krasevic M, et al. Frequency and distribution of lymph node metastases in epithelial ovarian cancer. *Int J Gynecol Cancer*. 2011;21:245–250.

24. McDonald SA. Principles of research tissue banking and specimen evaluation from the pathologist's perspective. *Biopreserv Biobank*. 2010;8:197–201. doi:10.1089/bio.2010.0018.

25. Roggli VL, Pratt PC. Numbers of asbestos bodies on iron-stained tissue sections in relation to asbestos body counts in lung tissue digests. *Hum Pathol*. 1983;14:355–361.

26. Leitje JAP, Valdes Olmos RA, Nieweg OE, et al. Anatomical mapping of lymphatic drainage in penile carcinoma with SPECT-CT: implications for the extent of inguinal lymph node dissection. *Eur Urol* 2008;54:885-890. doi:10.1016/j.euroro.2008.04.094.